MARCH 1983 LRP 219/83

PLASMA EQUILIBRIUM IN THE TCA TOKAMAK

F. Hofmann and B. Joye

PLASMA EQUILIBRIUM IN THE TCA TOKAMAK

F. Hofmann and B. Joye

Centre de Recherches en Physique des Plasmas

Association Euratom - Confédération Suisse

Ecole Polytechnique Fédérale de Lausanne

CH-1007 Lausanne / Switzerland

ABSTRACT

Plasma equilibria in the TCA tokamak have been computed using the 2D numerical code FBT. The effects of current peaking, density peaking and poloidal beta have been investigated. The results are compared with measurements on TCA.

1. INTRODUCTION

The TCA tokamak [1] was built in order to study Alfvén wave heating. It has been operating since 1980 and its main characteristics are as follows :

$R = 0.61$ m

$a \leq 0.18$ m

$B \leq 1.5$ T

$I \leq 135$ kA

Discharge duration is limited to $\sim$ 100 ms. Recent experiments [2] have shown that it would be very useful to be able to extend the pulse length up to 250 ms. In addition we may want to operate the machine at lower q and higher β values than are presently feasible. This will require an upgrade of the OH and B_V power supplies [3].

In order to investigate the implications of such modifications, we have performed equilibrium calculations covering wide ranges of parameters. In this report, we present the results of these calculations and compare them with measurements on TCA.

2. TCA POLOIDAL FIELD COIL SYSTEM

The vertical field in TCA is produced by a set of 8 coils placed symmetrically with respect to the mid plane [1]. The radii and

vertical positions of these coils are given in the table below :

Coil No	R[m]	Z[m]	Current
1	0.3325	0.048	I_v
2	0.3325	-0.048	I_v
3	0.3325	0.144	I_v
4	0.3325	-0.144	I_v
5	0.850	0.3525	$-I_v$
6	0.850	-0.3525	$-I_v$
7	0.935	0.1325	$-I_v$
8	0.935	-0.1325	$-I_v$

Note that all currents are equal in magnitude. The vertical field in vacuum at $R = R_0 = 0.61$ m, $Z = 0$ is given by

$$\frac{B_v}{I_v} = 3.606 \times 10^{-6} \quad \left[\frac{T}{A}\right]$$

The decay index at that point is

$$n = -\frac{R}{B_v}\frac{\partial B_v}{\partial R} = 0.45$$

Stray fields produced by the OH transformer are roughly two orders of magnitude less than the vertical field, hence they are neglected in this study.

3. NUMERICAL MODEL

The calculations described in this reprot were preformed by means of the FBT code, a free-boundary, 2-D tokamak equilibrium code developed recently at CRPP [4]. This code allows the prescription of arbitrary pressure and current profiles. For the purpose of this study we are using a family of profiles characterized by three parameters, l, m and α. These are defined by

$$p' = c_p \varphi^{\ell} \tag{1}$$

$$TT' = c_T \varphi^{m} \tag{2}$$

$$\alpha = \left[1 + \frac{c_T}{R_o^2 \mu_o c_p} \right]^{-1} \tag{3}$$

where

$$\varphi = \frac{\Psi - \Psi_{lim}}{\Psi_{ax} - \Psi_{lim}}$$

$$R_o = \frac{1}{2}(R_{LI} + R_{LO})$$

R_{LI} and R_{LO} are the inner and outer limiter radii, Ψ_{lim} and Ψ_{ax} are the values of Ψ at the limiter and on the magnetic axis, respectively, and c_p and c_T are constants.

The three parameters ℓ, m, and α determine the physical parameters of the system, i.e., current profile, density profile and poloidal beta.

The poloidal beta is defined as

$$\beta_p = \frac{8\pi \iint p \, ds}{\mu_0 I^2} \tag{4}$$

The current profile is related to the ratio (q_a/q_0) where the q's are defined by

$$q_a = \frac{2\pi a^2 B_0}{\mu_0 R_0 I} \tag{5}$$

$$q_0 = \frac{2 B_{ax}}{\mu_0 R_{ax} j_{ax}} \tag{6}$$

Here, B_0 is the toroidal vacuum field at $R = R_0$, B_{ax} and j_{ax} are the toroidal field and current density on the magnetic axis, and R_{ax} is the radius of the magnetic axis. The value of B_0 is irrelevant for the equilibrium calculation, however, it may be computed by assuming $q_0 = 1$.

The density profile, on the other hand, is usually characterized by an exponent, κ_ρ. The definition of κ_ρ in a toroidal equilibrium, however, is not obvious. In analogy to the case of a straight cylinder, where one generally assumes

$$\rho = \rho_0 \left[1 - \left(\frac{r}{a}\right)^2\right]^{\kappa_\rho}$$

we define κ_p as follows

$$\left.\begin{aligned} \varkappa_p &= \varkappa_p - \frac{2}{3}\varkappa_j \\ \varkappa_p &= \frac{\ln 0.5}{\ln\left[1-\left(\frac{w_p}{2a}\right)^2\right]} \\ \varkappa_j &= \frac{\ln 0.5}{\ln\left[1-\left(\frac{w_j}{2a}\right)^2\right]} \end{aligned}\right\} \quad (7)$$

where w_p and w_i are the full widths at half maximum of the pressure and current profiles (at z = 0), and 2a is the radial extent of the plasma (at z = 0).

Equilibrium calculations were performed using various combinations of the parameters ℓ, m and α and in each case, the physical parameters (q_a/q_0), κ_p and β_p were evaluated. This allows us to find relationships between the mathematical and physical parameters and to predict the values of ℓ, m and α which are necessary to produce a given set of values (q_a/q_0), κ_p and β_p.

First of all, we find that β_p is a function of α, as is shown in Fig. 1. This function can be written approximately as

$$(A-\beta_p)(\alpha+A-1) = A(A-1) \quad (8)$$

where A is a constant depending on ℓ and m. When ℓ = m, A becomes very large and β_p is nearly equal to α. Some values of A are given in the Table below :

ℓ	m	A
1	1.5	2.901
1	2	1.835
1	2.5	1.495
1	3	1.333
1.5	2	3.145
2	2	27.873
2	2.5	3.327
2	3	2.105

Eq. (8) reproduces the true functions β_p (α), as shown in Fig. 1, to within about 2%.

Fig. 2 shows how (q_a/q_0) and β_p depend on m and α for constant ℓ. When ℓ is increased, we obtain qualitatively the same picture but displaced towards higher values of (q_a/q_0). Fig. 3 on the other hand shows κ_p and β_p as functions of m and α for constant ℓ. Again, for larger ℓ, the results are similar but displaced towards higher values of κ_p.

4. RESULTS

All calculations presented in this report are based on the TCA poloidal field system, as described in section 2, and we assume two rail limiters at R_{LI} = 0.43 and R_{LO} = 0.79 m.

4.1 Currents in Vertical Field Coils

Traditionally, the vertical field in a tokamak is computed analytically from the Shafranov equation

$$\frac{B_v}{I_p} = \frac{\mu_o}{4\pi R_o}\left[\ln\frac{8R_o}{a} + \beta_p + \frac{\ell_i}{2} - \frac{3}{2}\right] \quad (9)$$

which is based on a large aspect ratio expansion. The quantity ℓ_i can be expressed in terms of q_a/q_0 if one assumes a current density profile of the form

$$j = j_o\left[1 - \left(\frac{r}{a}\right)^2\right]^{x_j} \quad (10)$$

We then have

$$\ell_i = 2\int_0^1 \left[1 - \left(1-x^2\right)^{x_j+1}\right]^2 \frac{dx}{x} \quad (11)$$

where

$$x_j = \frac{q_a}{q_o} - 1 \quad (12)$$

For TCA parameters (R_0 = 0.61, a = 0.18, B_v = 3.606 x 10^{-6} I_v) we obtain the results shown in Fig. 4 (dashed lines).

More accurate values can be obtained from the 2-D equilibrium calculations. In this case, the vertical field is determined by the condition that the outermost flux surface must coincide with the two limiters (R_{LI} = 0.43, R_{LO} = 0.79) at the midplane (z = 0). The results are shown as solid lines in Fig. 4.

The small discrepancy between analytical and numerical results is due to toroidal effects and may be explained as follows : The radius R_0 in eq. (9) is assumed to be constant and equal to the mean plasma radius, $R_0 = 0.5\ (R_{LI} + R_{LO})$. In fact, R_0 should not be taken as constant since the magnetic axis is shifted outward and its radius depends on β_p and q_a/q_0, as will be shown below. If one uses the radius of the magnetic axis, instead of R_0, in eq. (9) one obtains much better agreement with the numerical calculation.

Results of measurements on TCA are also shown in Fig. 4. They agree with the theoretical curves, within experimental error.

4.2 Radial displacement of the Magnetic Axis

Fig. 5 shows the outward shift of the magnetic axis, $\Delta R = R_{ax} - R_0$, as a function of β_p for two different values of q_a/q_0. Experimental values, obtained from radial temperature profiles, are also shown in the Figure, giving the displacement of magnetic axis with respect to the geometric axis. This implies a good centering of the limiting surface which is not measured on TCA.

4.3 Effect of Density Peaking

In Fig. 6 we plot the results of three equilibrium calulations with identical values of β_p and q_a/q_0 but different values of κ_p. It

is interesting to see that both the current in the vertical field coils (I_V/I_p) as well as the total poloidal flux (Ψ_{ax}) are strictly independent of κ_ρ. The radial shift, ΔR, exhibits a slight dependence on the density profile, whereas the maximum plasma pressure grows rapidly with increasing κ_ρ.

4.4 Relationship between q_a and q_Ψ

The "true" value of q is defined as

$$q_\psi = \frac{T}{2\pi} \oint \frac{d\ell}{R|\nabla\psi|} \qquad (13)$$

where $T = RB_\phi$ and $d\ell$ is a line element, parallel to a poloidal field line. q_Ψ is always larger than q_a (eq. 5) due to toroidal geometry. Fig. 7 shows q_Ψ evaluated on the outermost flux surface, as a function of q_a, for various values of β_p. An approximate formula is given below :

$$(q_\psi - 0.672) = (q_a - 0.608)\left(1.124 + 0.0533\,\beta_p^{1.67}\right) \qquad (14)$$

Within the parameter ranges covered by this study ($0 < \beta_p < 1.8$, $1.7 < q_a < 8$), the accuracy of eq. (14) is better than 1%.

4.5 Flux Surfaces, Radial Profiles, β-values

In order to illustrate the effects of β_p and current peaking on the structure of the equilibrium, we have computed four cases with rather extreme parameters. The results are summarized in the Table, below :

Case		1	2	3	4
β_p		0.1528	1.685	0.1353	1.829
q_a/q_0		2.182	1.788	6.602	5.827
β[%]		0.280	4.589	0.027	0.470
β_{max}[%]		0.826	13.59	0.209	3.712
B_0=1.16	I_p[kA]	141.2	172.3	46.7	52.9
	I_v [kA]	15.5	29.3	5.9	10.3
	n^*_{max} $*10^{-19}$	1.38	22.7	0.35	6.21
B_0=1.51	I_p[kA]	183.8	224.3	60.7	68.9
	I_v[kA]	20.2	38.2	7.7	13.4
	n^*_{max} $*10^{-19}$	2.34	38.5	0.59	10.52
FIGURE		8	9	10	11

* maximum densities are computed by assuming $Te_{max} = Ti_{max}$ = 1 KeV and Z_{eff} = 1.

Note that average β-value of 4.5 % can be reached at very low q and high β_p (case 2). The vertical field currents which are necessary to achieve this, however, are considerably larger than those which are presently available ($I_V \leq 20$ kA).

Figs. 8-11 show the poloidal flux surfaces as well as the radial profiles of pressure and current density for the four cases listed above. Corresponding q-profile are shown in Fig. 12.

5. ACKNOWLEDGEMENTS

The authors wish to acknowledge useful discussions with Dr. K. Lackner.

REFERENCES

[1] A.D. Cheetham et al., Proc. 11th Symp. on Fusion Technology, Oxford 1980, Vol. 1, p. 601.

[2] A. De Chambrier et al., Proc. 9th Int. Conf. on Plasma Physics and Controlled Nuclear Fusion Research, Baltimore 1982, IAEA-CN-41, Paper J-1-1.

[3] F. Hofmann and A. Tuszel, "Upgrade of OH and Vertical Field Power Supplies of TCA", Application for Euratom Preferentiel Support, Janv. 1983.

[4] F. Hofamnn, CRPP INT 110/82

FIGURES CAPTIONS

Fig. 1 β_p as a function of α and m, for $\ell = 1$.

Fig. 2 β_p and (q_a/q_0) as functions of α and m, for $\ell = 1$.

Fig. 3 β_p and κ_p as functions of α and m, for $\ell = 1$.

Fig. 4 Vertical field current, I_v/I_p as a function of β_p and (q_a/q_0).

Fig. 5 Radial shift ΔR as a function of β_p and (q_a/q_0).

Fig. 6 Effect of density peaking on maximum plasma pressure (p_{max}), vertical field current (I_v/I_p), poloidal flux (Ψ_{ax}) and radial shift (ΔR).

Fig. 7 q_Ψ as a function of q_a and β_p.

Fig. 8 Low-β, low-q TCA equilibrium.

Fig. 9 High-β, low-q TCA equilibrium.

Fig. 10 Low-β, high-q TCA equilibrium.

Fig. 11 High-β, high-q TCA equilibrium.

Fig. 12 q-profiles of the equilibria shown in Figs 8-11.

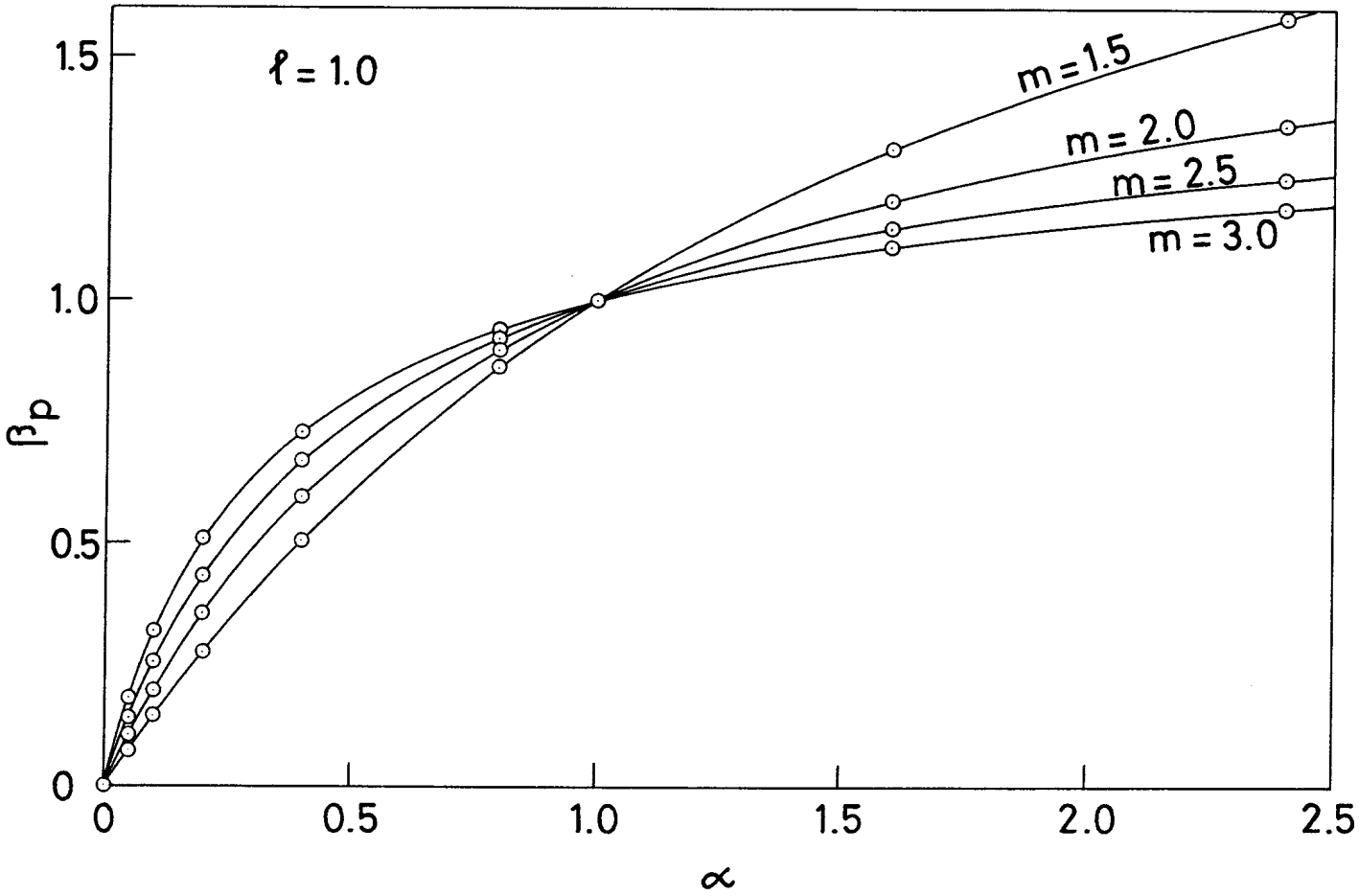

FIG.1

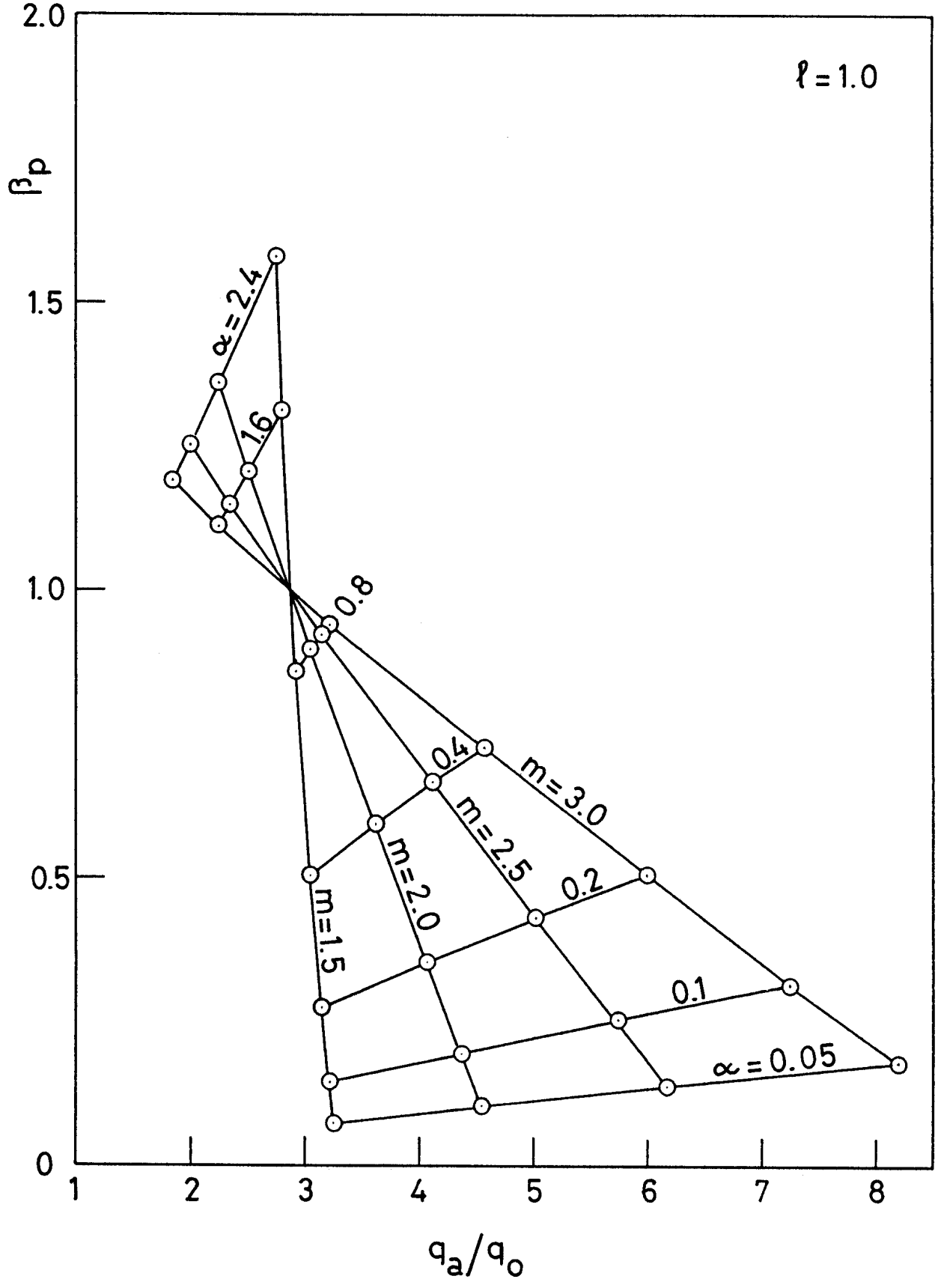
2.0
1.5
1.0
0.5
0
β_p
$\ell = 1.0$
$\alpha = 2.4$
1.6
0.8
0.4
0.2
0.1
$\alpha = 0.05$
m=3.0
m=2.5
m=2.0
m=1.5
1
2
3
4
5
6
7
8
q_a/q_o

FIG. 2

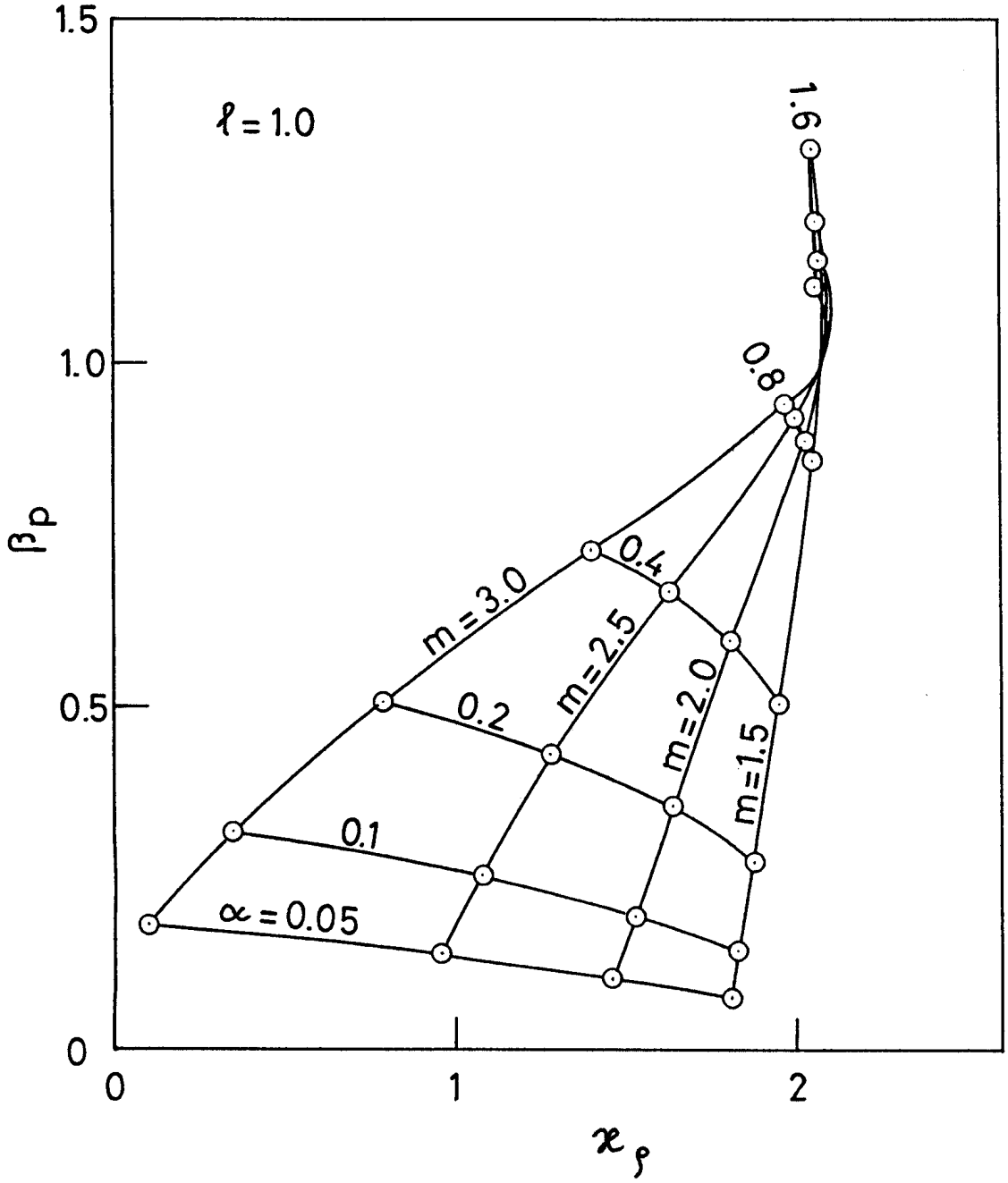
1.5
1.0
0.5
0
0
1
2
β_p
x_s
$\ell = 1.0$
1.6
0.8
0.4
0.2
0.1
$\alpha = 0.05$
m=3.0
m=2.5
m=2.0
m=1.5

FIG. 3

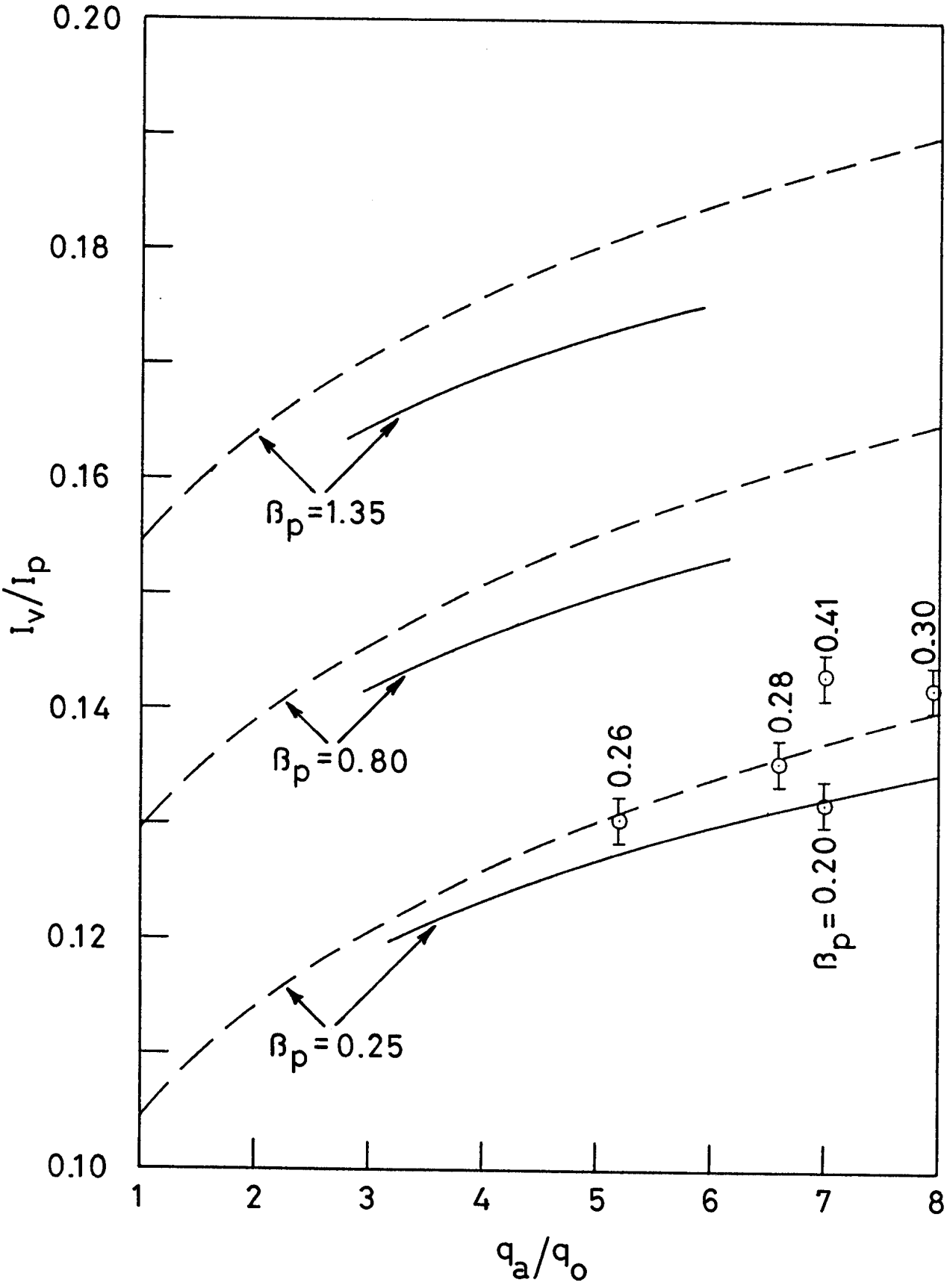
0.20
0.18
0.16
0.14
0.12
0.10
I_v/I_p
1
2
3
4
5
6
7
8
q_a/q_o
$\beta_p = 1.35$
$\beta_p = 0.80$
$\beta_p = 0.25$
$\beta_p = 0.20$
0.26
0.28
0.41
0.30

FIG. 4

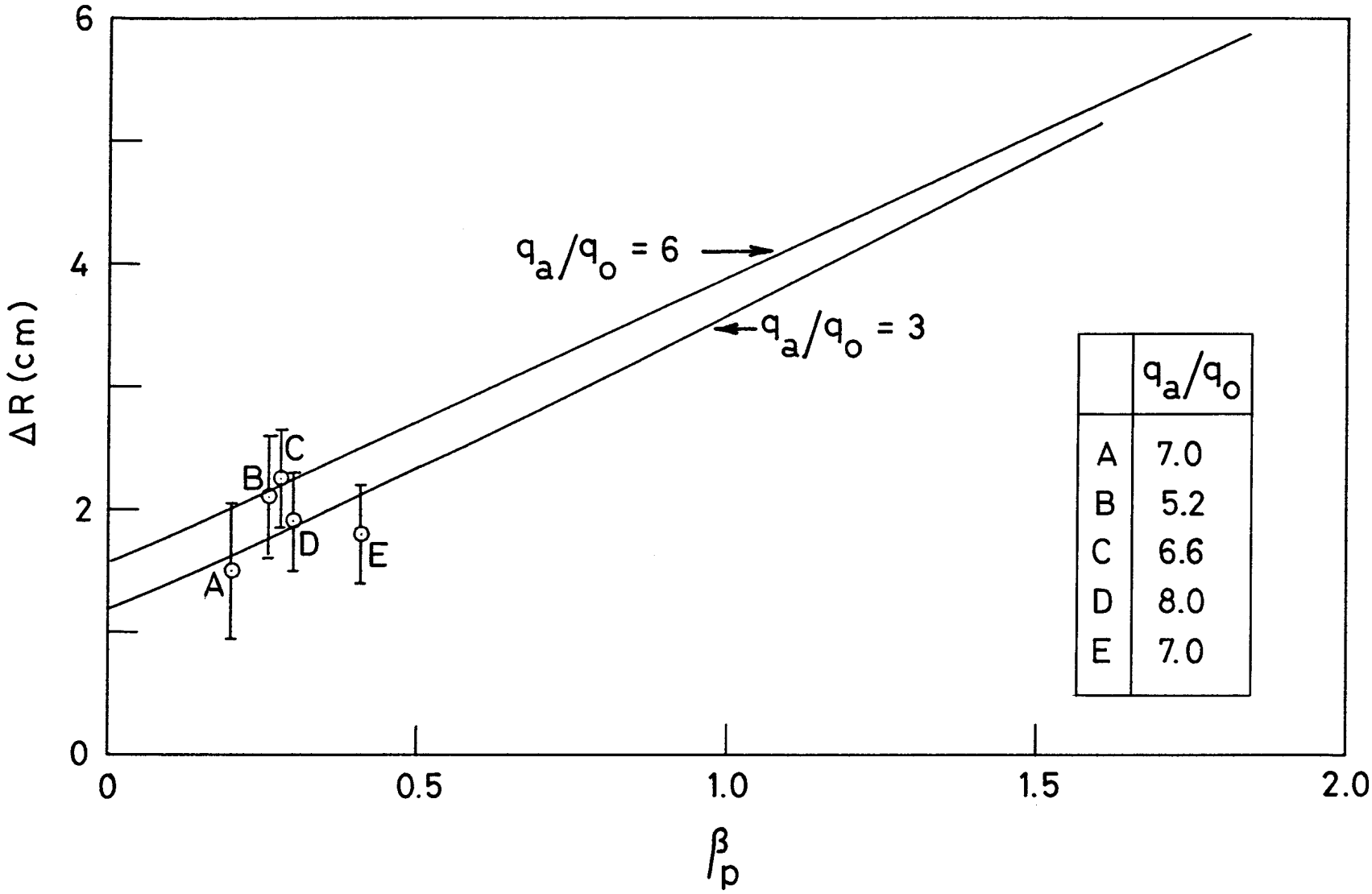
6
4
2
0
ΔR (cm)
0
0.5
1.0
1.5
2.0
β_p
$q_a/q_o = 6$
$q_a/q_o = 3$
A
B
C
D
E
q_a/q_o
A 7.0
B 5.2
C 6.6
D 8.0
E 7.0

FIG. 5

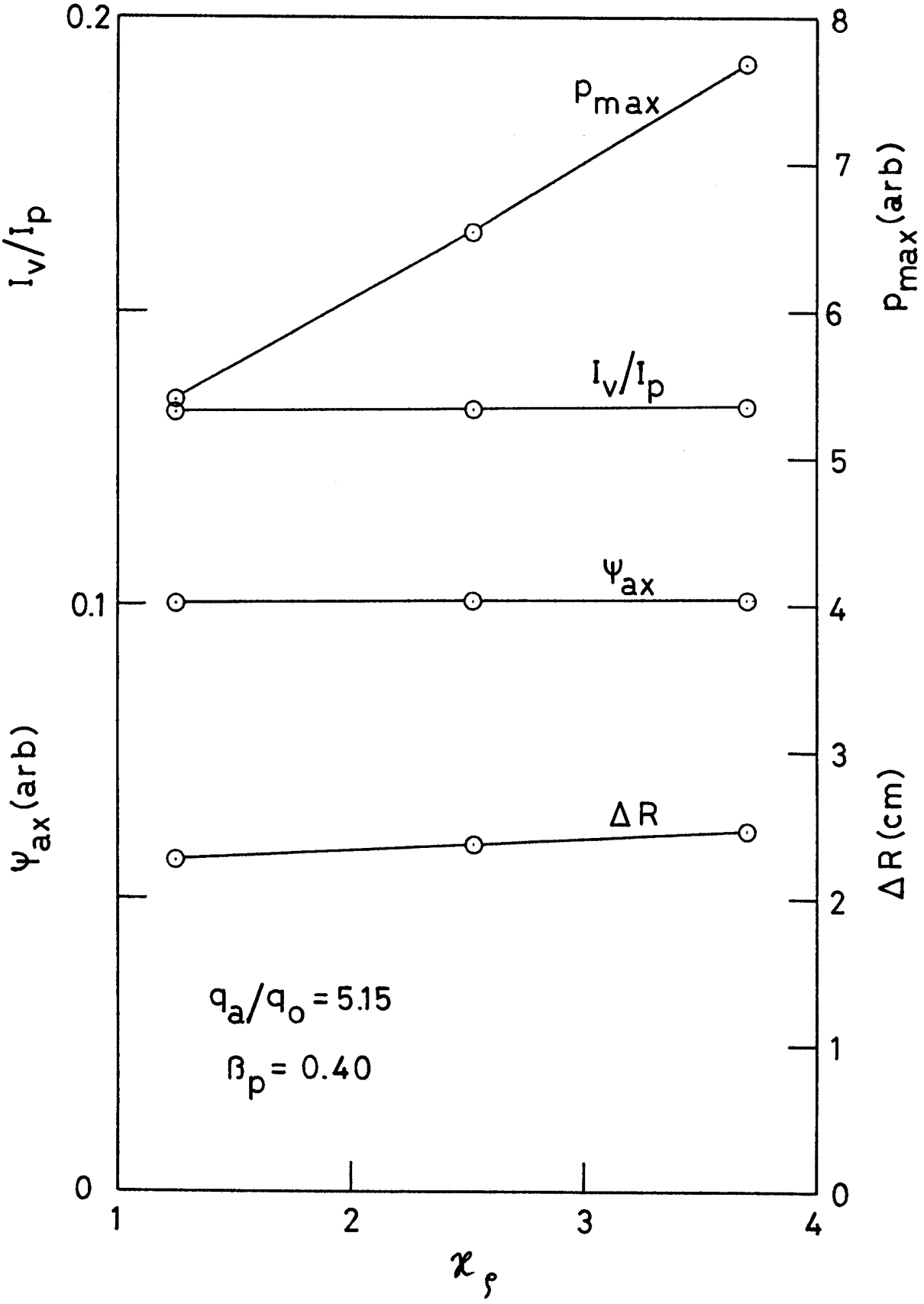
0.2
0.1
0
1
2
3
4
8
7
6
5
4
3
2
1
0
I_v/I_p
ψ_{ax}(arb)
p_{max}(arb)
ΔR(cm)
p_{max}
I_v/I_p
ψ_{ax}
ΔR
$q_a/q_o = 5.15$
$\beta_p = 0.40$
ρ

FIG. 6

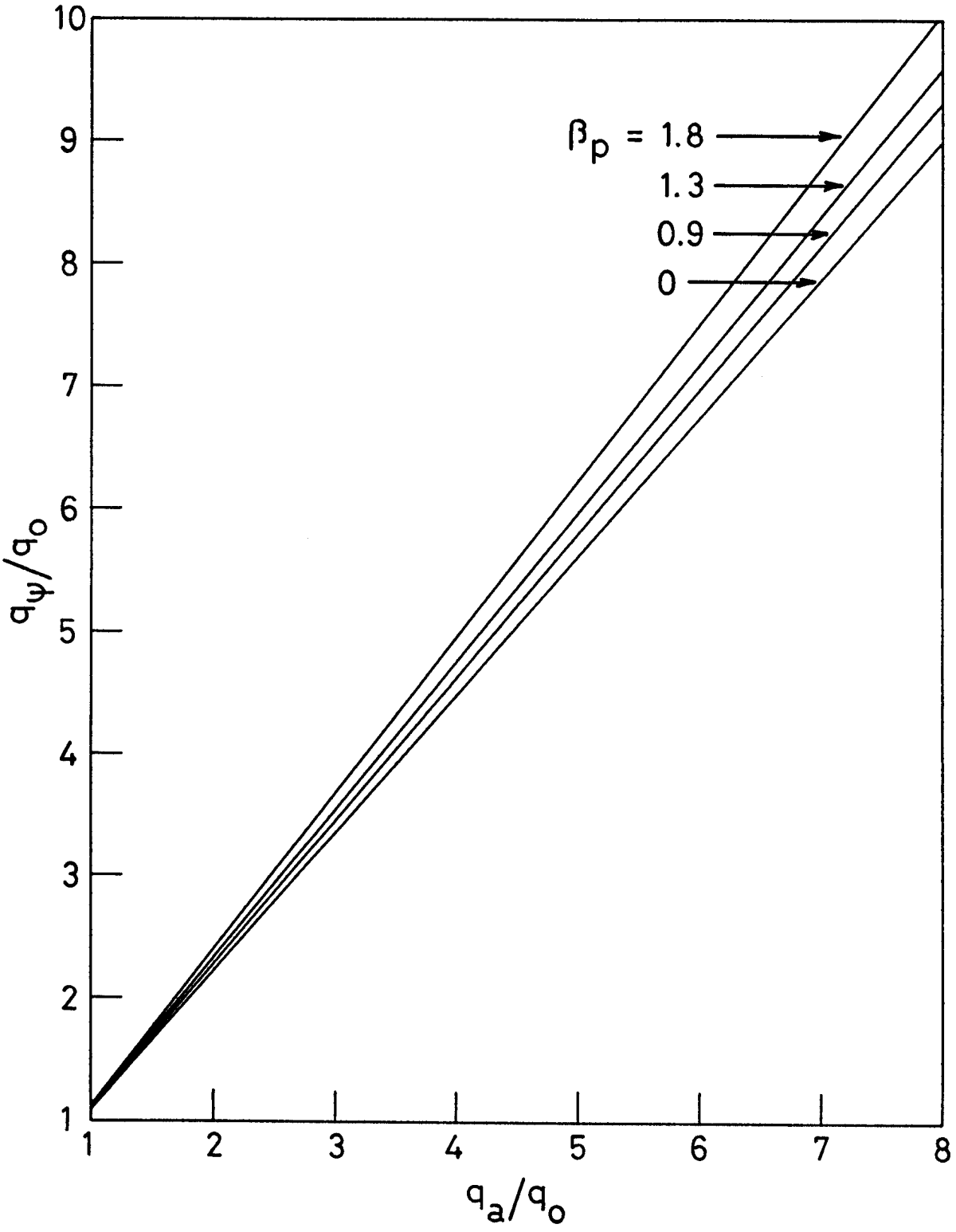

FIG. 7

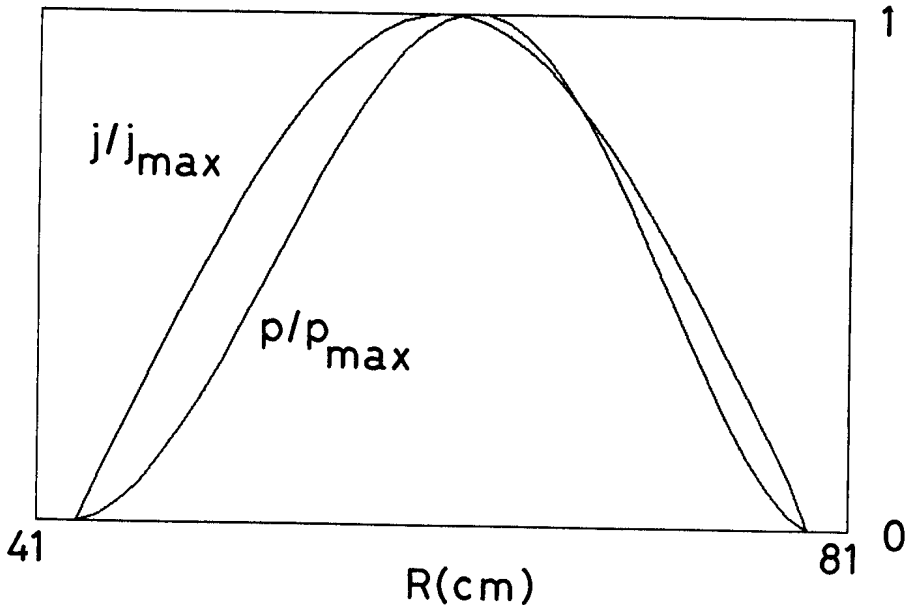

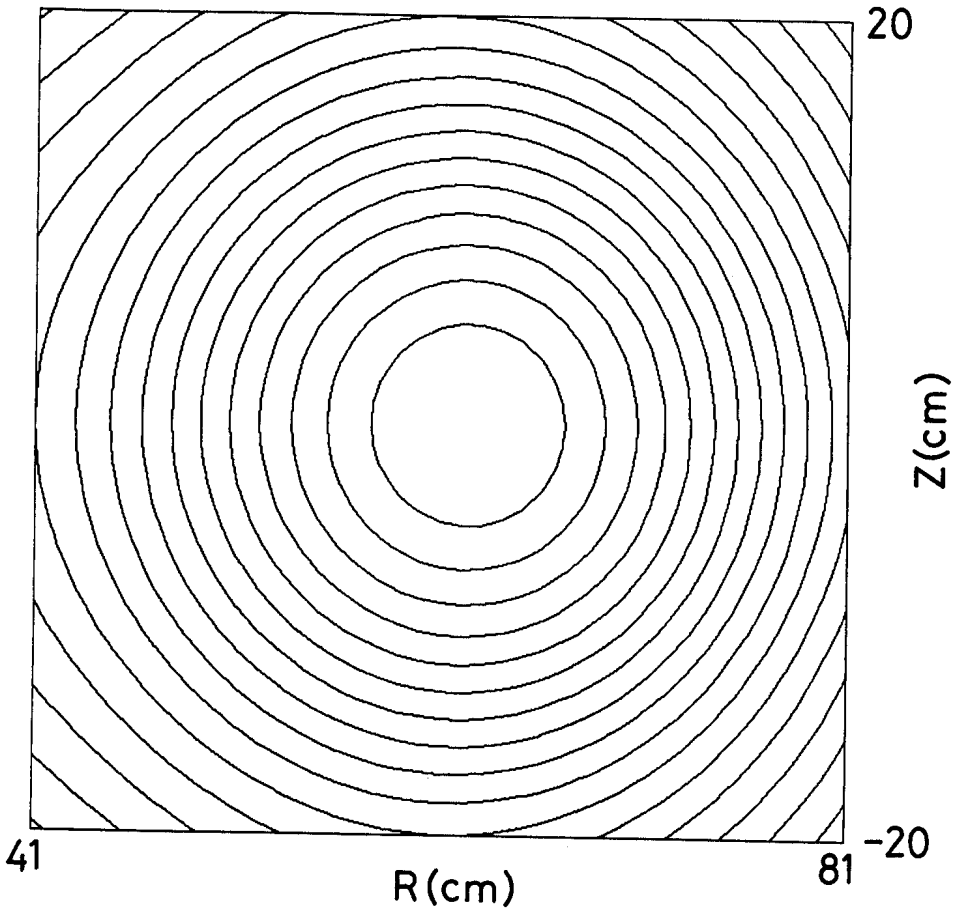

FIG. 8

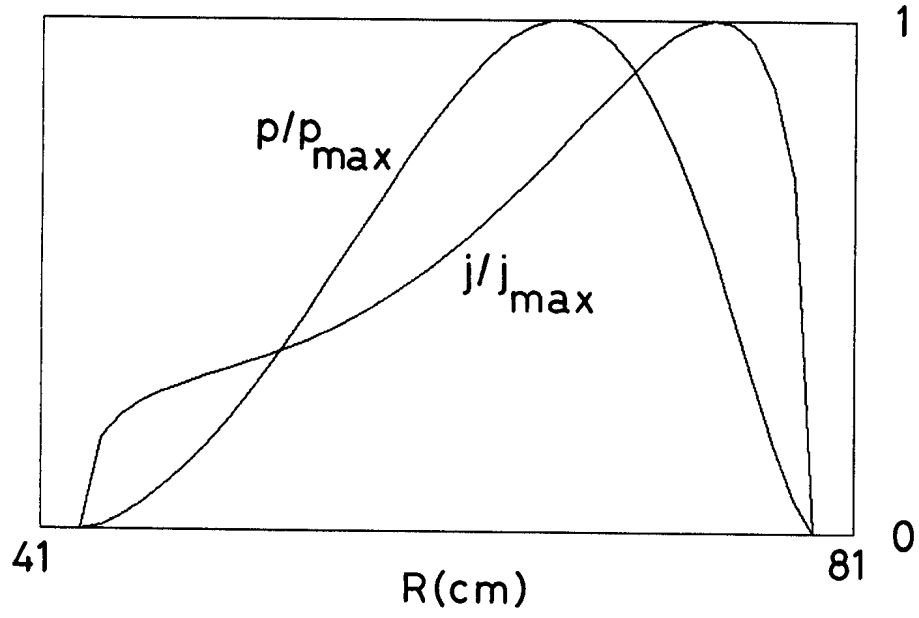

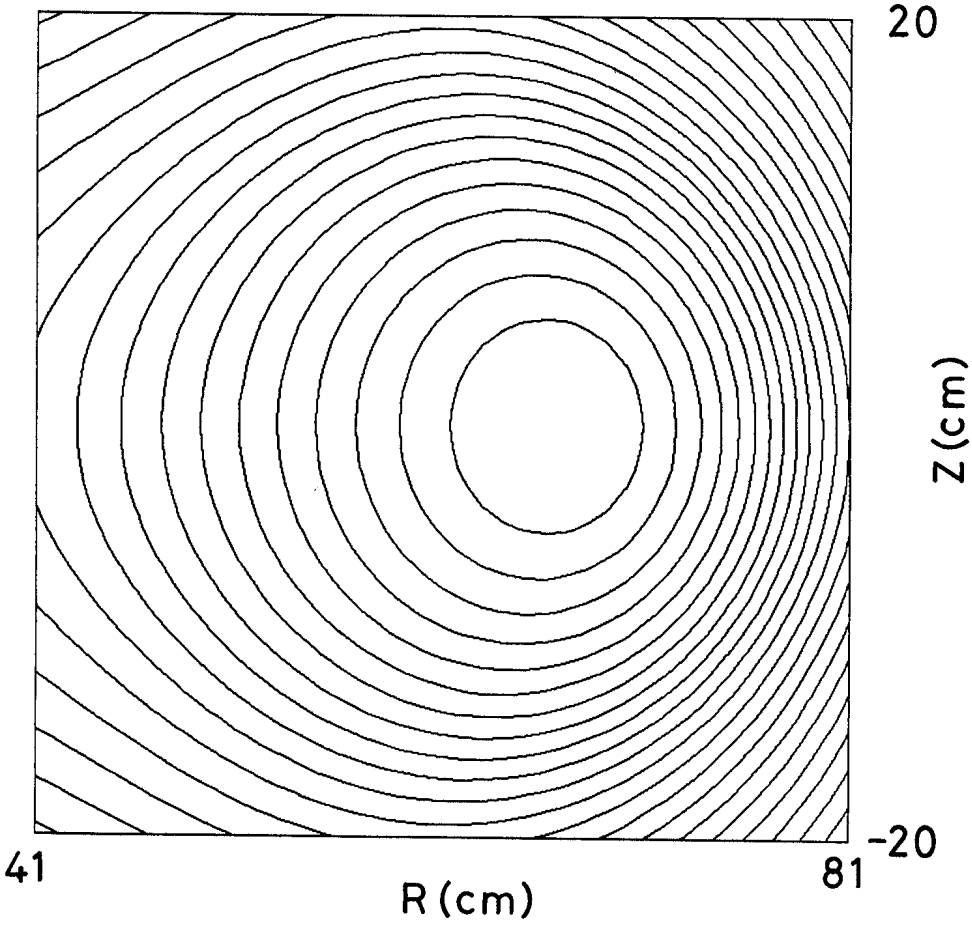

FIG. 9

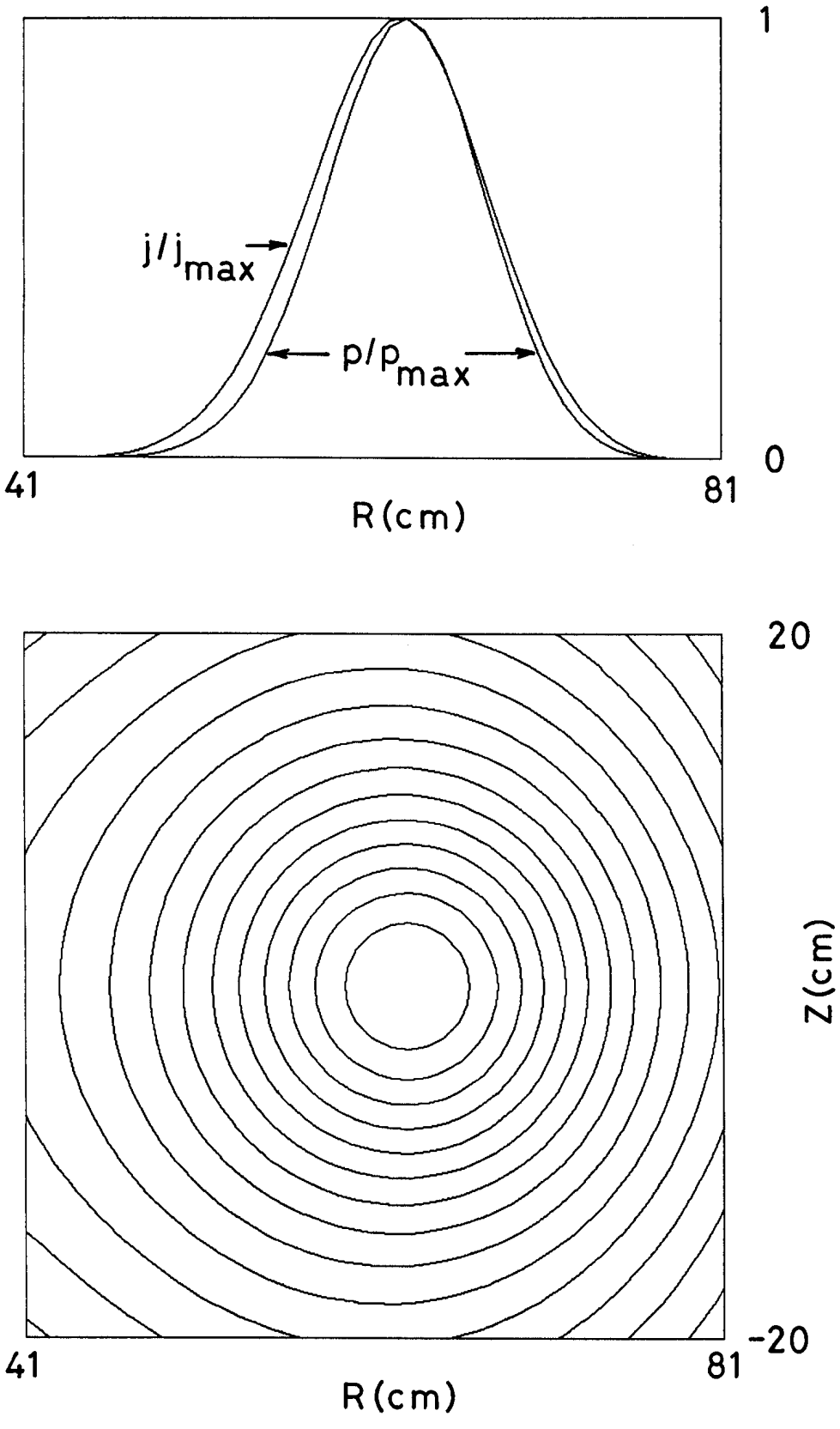

FIG. 10

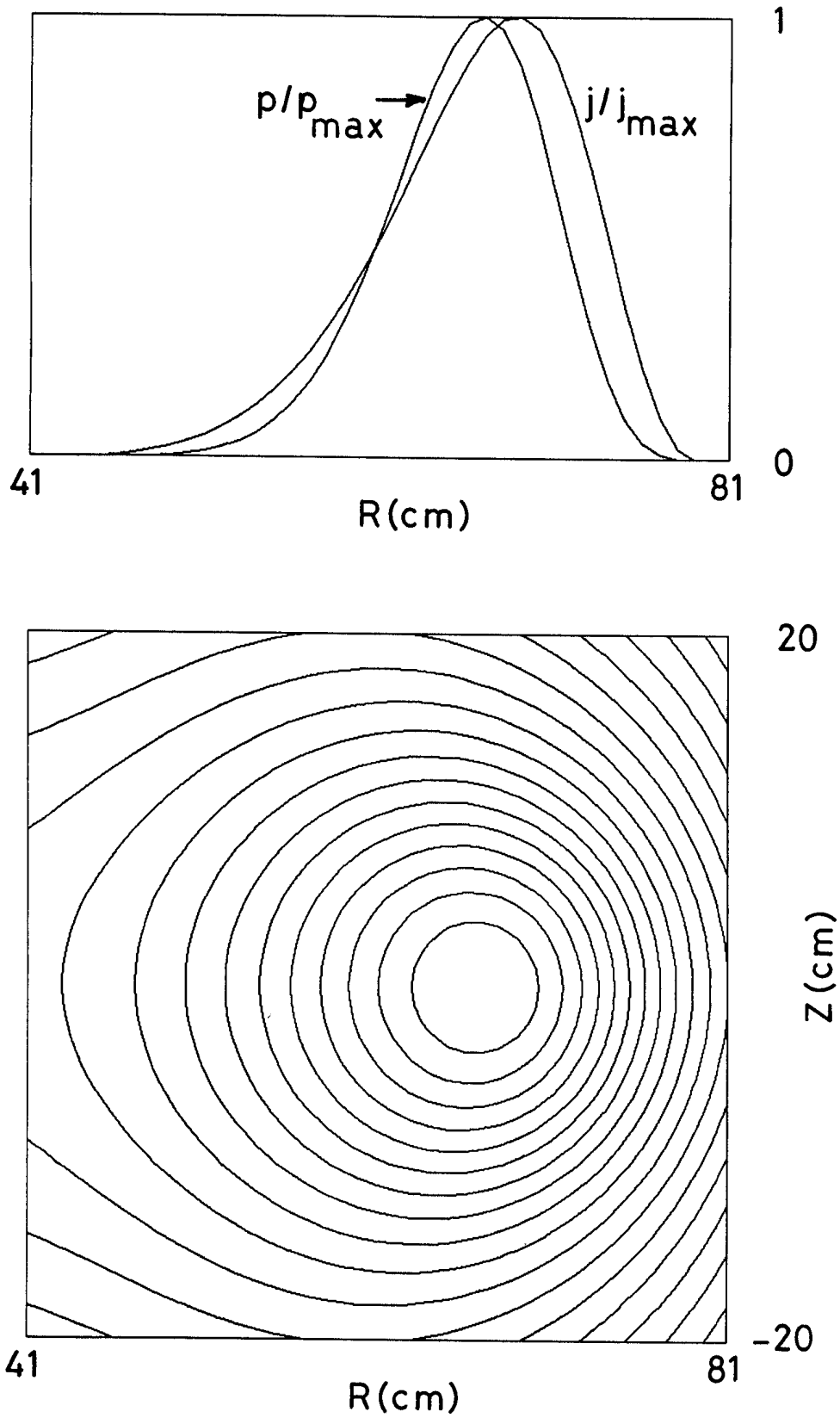

FIG. 11

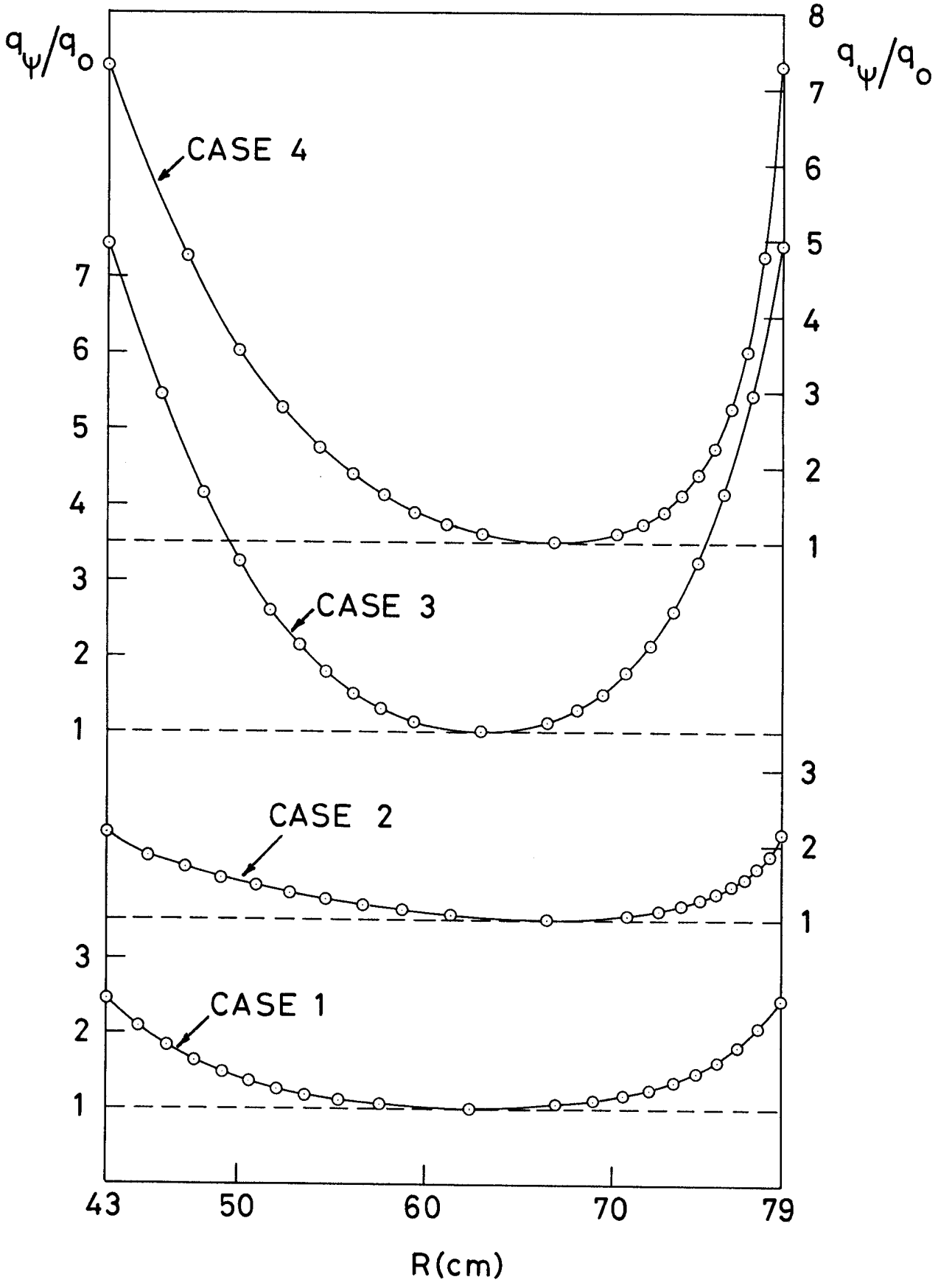
q_ψ/q_o
q_ψ/q_o
CASE 4
CASE 3
CASE 2
CASE 1
8
7
6
5
4
3
2
1
43
50
60
70
79
R(cm)

FIG. 12